Dissecting Processing and Apoptotic Activity of a Cysteine Protease by Mutant Analysis

Bernard Allet, Alena Hochmann, Isabelle Martinou, Anouk Berger, Marc Missotten, Bruno Antonsson, Rémy Sadoul, Jean-Claude Martinou, and Lilia Bernasconi

Geneva Biomedical Research Institute, Glaxo Wellcome Research and Development S.A., 14 1228 Plan-Les-Ouates, Geneva, Switzerland

Abstract. We have compared the behavior of wild-type mouse NEDD-2, a neural precursor cell–expressed, developmentally down-regulated cysteine protease gene, to various mutant forms of the gene in both apoptotic activity in neuronal cells and proteolytic cleavage in the Semliki Forest virus and rabbit reticulocyte protein expression systems. Our results confirm that NEDD-2 processing and apoptotic activity are linked phenomena. They identify aspartate residues as likely targets for autocatalytic cleavage. They establish that cleavage events only occur at specific sites. Finally, they pinpoint differential effects of individual mutations on the overall proteolytic cleavage patterns, raising interesting questions related to the mechanisms of subunit assembly.

Over the past two years, proteolysis has emerged as an important mechanism underlying programmed cell death (PCD).[1] A major step toward the development of this concept has been the discovery of structural homology between interleukin (IL)-1β converting enzyme (ICE), a protease involved in the processing of IL-1β precursor in monocytes, and ced-3, a protein required for cells to undergo PCD in the nematode *Caenorhabditis elegans* (Yuan et al., 1993). ICE and ced-3 are prototypes of a family of cysteine proteases to which were added ICH-1/NEDD-2 (Kumar et al., 1994; Wang et al., 1994), CPP32/YAMA/Apopain (Fernandes-Alnemri et al., 1994; Tewari et al., 1995; Nicholson et al., 1995), TX/Ich-2/ICEIII (Munday et al., 1995; Faucheu et al., 1995; Kamens et al., 1995), Mch2 (Fernandes-Alnemri et al., 1995*a*), and Mch3/ICE LAP3 (Fernandes-Alnemri et al., 1995*b*; Duan et al., 1996). There are several reasons to believe that these proteases play a role in PCD: (*a*) their overexpression was shown to trigger PCD in diverse cell types (for review see Yuan, 1995); (*b*) viral protein CrmA and p35, from cowpoxvirus and baculovirus, respectively, can inhibit catalytic activity of different members of this gene family, and thereby block PCD (Bump et al., 1995; Xue and Horvitz, 1995; Martinou et al., 1995; Gagliardini et al., 1994); and (*c*) poly (ADP-ribose) polymerase and U1-70 K proteins, two substrates of these proteases, are cleaved early in PCD (for review see Martin and Green, 1995).

Most of the knowledge about the mechanism of action of cysteine proteases comes from studies on ICE. The ICE gene product is a 45-kD proenzyme that requires proteolytic processing for activation (Thornberry et al., 1992; Ceretti et al., 1992). Four internal proteolytic cleavage sites at aspartate residues have been identified by protein sequencing (Thornberry et al., 1992), resulting in the removal of an 11-kD NH_2-terminal precursor domain and of an internal 19–amino acid sequence with concomitant production of two subunits of 20 and 10 kD. The crystal structure of active ICE revealed that the protease is a tetramer of two p20 subunits surrounding two adjacent p10 subunits that form the dimer–dimer interface. The active site of ICE comprises amino acid residues from both p20 and p10 polypeptides (Walker et al., 1994; Wilson et al., 1994; Gu et al., 1995).

Structural homologies between members of the ICE family of proteases include a characteristic QACRG motif containing the catalytic cysteine residue (C285), and an array of aspartate residues, some of which are presumably targets for intramolecular cleavages. In ICE, a role for the C285 residue in catalytic activity has been reported by Thornberry et al. (1992). In NEDD-2, the corresponding cysteine residue (C319) was shown to be required for apoptotic activity (Wang et al., 1994; Kumar et al., 1994), suggesting that it was, indeed, the protease activity of this gene that was responsible for mediating cell death. To date, however, there have been no reports on the effects of mutations at the aspartate residues involved in intramolecular cleavages.

Address all correspondence to Bernard Allet, Geneva Biomedical Research Institute, Glaxo Wellcome Research and Development S.A., 14, chemin des Aulx, 1228 Plan-Les-Ouates, Geneva, Switzerland. Tel.: (41) 22 706 9666. Fax: (41) 22 794 6965.

1. *Abbreviations used in this paper*: ICE, interleukin-1β converting enzyme; IL, interleukin; mut, mutant; PCD, programmed cell death; SFV, Semliki Forest virus; WT, wild type.

In this paper we describe a series of mutants of NEDD-2 that affect either the catalytic cysteine or various aspartate residues, and we have analyzed the ability of these mutants to promote an apoptotic response in primary cultures of neuronal cells. In parallel, we have compared the proteolytic cleavage products of the same mutants in two different test situations: (*a*) overexpression in CHO cells driven by the Semliki Forest virus system and (*b*) the acellular rabbit reticulocyte expression system. Our results lead to several conclusions. First, they show that proteolytic cleavages occurring on both sides of the p20 subunit are necessary for biological activity. In addition, they identify aspartate residues that are targets for intramolecular cleavages and confirm specificity of these target sites by eliminating the possibility that alternative cleavage sites may be efficiently occurring. Finally, they pinpoint differential effects of mutations on the overall cleavage patterns.

Materials and Methods

Plasmids and Bacteria

Plasmids were propagated in *Escherichia coli* C600 (λ) and purified by standard procedures (Maniatis et al., 1982). For expression under pL promoter, the plasmid constructs (Fig. 1 *A*) were transferred into *E.coli* B, a natural lon-prototroph (Allet et al., 1988). Plasmids pSFV-1 and pSFV-2-helper (Liljestrom and Garoff, 1991) were provided by K. Lundstrom (Roche Institute, Basel, Switzerland), pEE12 (Bebington and Hentschel, 1987) was provided by C.R. Bebington (Celltech Ltd., Berkshire, UK), and pSP73 was purchased from Promega (Madison, WI).

Cell Lines and Primary Cultures

BHK-21 and CHO cell lines from the American Type Culture Collection (Rockville, MD) were grown in Ham's F-12/ basal Iscove medium in a 1:1 ratio (Seromed, Biochrom KG, Berlin, Germany) containing 10% FCS and 4 mM glutamine. Sympathetic neuron primary cultures were established from superior mouse cervical ganglia and cultured as described previously (Garcia et al., 1992).

Cloning, PCR Technology, and Mutagenesis

Enzymatic manipulations of DNA with restriction enzymes, calf intestine alkaline phosphatase, polynucleotide kinase, T4 DNA ligase, and T7 and SP6 RNA polymerases were as recommended by the suppliers. Basic methods of genetic engineering (gene cloning, purification of fragments, ligations, PCR technology) were according to standard protocols (Ausubel et al., 1992).

Oligonucleotides were prepared in an automated DNA synthesizer (ABI 394; Applied Biosystems, Foster City, CA) using the phosphoamidite chemistry according to the instructions recommended by the suppliers.

The NEDD-2 mutants were prepared by a PCR methodology. The template was wild type pEE12-NEDD-2 (Fig. 1 *B*) used in a sufficient amount (50 ng) to reduce the number of cycles in DNA amplification to 20. A common set of two synthetic oligonucleotides was used to prepare all the mutants. One oligonucleotide ① corresponded to sequences in the upper strand, in a region upstream from the unique SacI site, and the other, in the lower strand ②, in a region downstream from the XbaI site at the translation termination site. The lengths of these oligonucleotides were adapted to exhibit a melting temperature between 60° and 64°C, assuming a melting temperature of 2°C for each A-T, and of 4° for each G-C base pairing. For each individual mutant, a set of two complementary oligonucleotides harboring the selected base alteration in the middle was synthesized (③ and ④, upper and lower strand, respectively). In designing these oligonucleotides, a melting temperature of 30°–34°C was selected on each side of the mutated base. Two PCR reactions were set up, one with each of the mutated oligonucleotides combined with the appropriate common oligonucleotide (i.e., ④-① and ③-②). The resulting amplified fragments were purified, combined (50 ng each), and used as template for a second round of PCR amplification using the set of common oligonucleotides (① and ②). The amplified fragments were digested with a mixture of SacI and XbaI restriction enzymes, and the fragments were purified and cloned back in the original plasmid DNA by standard procedures. All constructs were confirmed by DNA sequencing.

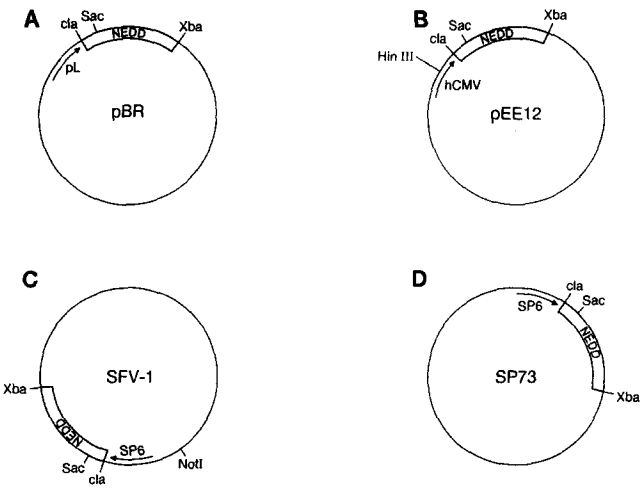

Figure 1. Expression plasmids. Plasmid pBR (*A*) is for expression in *E. coli*, pEE12 (*B*) in neuronal cells, SFV-1 (*C*) in the Semliki Forest virus system, and SP73 (*D*) in the rabbit reticulocyte system. Promoters are indicated and characteristic restriction sites (not necessarily unique) used in constructions are shown.

The residue Cys 320, present in the QACRG motif and assumed to be essential for the protease activity, was mutated to Ala. By analogy with other members of the cysteine protease gene family, catalytic cleavage sites must exist at aspartate residues to generate the so-called p20 and p10 subunits that assemble to form the active protein (Wilson et al., 1994). The position of such residues in NEDD-2 was unknown, but Kumar et al. (1994) had identified numerous potential candidates (aspartate D100, D116, D124, D135, D137, D159, D326, D330, D333, D347, and D362) on the basis of homologies with ICE. We have selected some of them together with a few others for mutagenesis into Ala residues (Fig. 2). In parallel, we used a PCR-based procedure to construct three fragments assumed to encode both p20 and p10 (T138 to T452), p20 only (T138 to D333), or p10 only (A348 to T452), possibly fused to the linker sequence between p20 and p10. The various mutants and gene fragments are shown in Fig. 2. They were subcloned into the plasmids shown in Fig. 1, *A–D*.

Polyclonal Antibodies against p20

The NEDD-2 sequences from threonine 138 to aspartate 333, presumed to include the p20 subunit, were amplified by PCR. The synthetic oligonucleotide at the amino terminus had a tail ending with a ClaI followed by an NdeI site (...ATCGATTCATATG). On the opposite strand the oligonucleotide had a tail ending with a XbaI site followed by the CTA triplet corresponding to the translation termination site. The amplified DNA was digested by the mixture of ClaI and XbaI restriction enzymes and subcloned into the corresponding sites of the pL plasmid (Fig. 1 *A*). The plasmid was propagated in C600 (λ), transformed into *E.coli* B, and heat induced for expression. High expression was observed (~20% of total protein mass), and the polypeptide of 20 kD was found in the insoluble fraction (inclusion bodies) after sonication followed by centrifugation. This insoluble pellet from 1 L induced culture (~1 g of wet cells) was dissolved in SDS-PAGE sample buffer and loaded on a preparative 18% gel. After electrophoretic migration, the protein band of 20 kD was electroeluted in SDS-PAGE buffer, and the eluates (20–50 μg/ml) were used to raise polyclonal antibody in rabbits (Neosystems, Strasbourg, France).

Efforts to prepare antibodies against p10 (A348 to T452) were unsuccessful because upon heat induction, the p10 polypeptide was degraded into smaller products. We have not attempted to recover these degradation products.

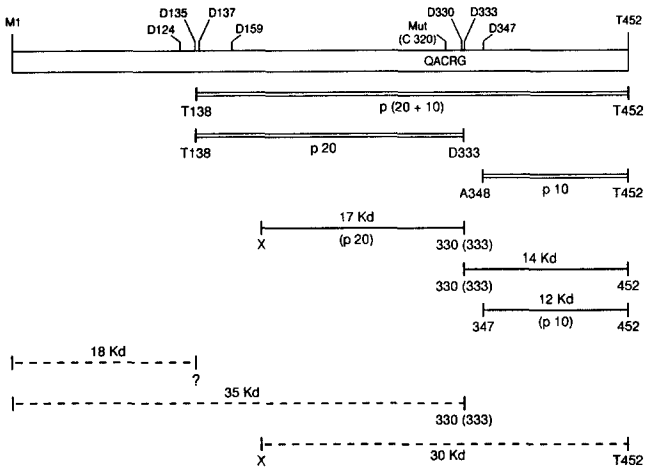

Figure 2. Physical map of mutants and fragments. The figure summarizes mapping data on point mutants and on fragments that were either deliberately synthesized or were produced during processing in the SFV and rabbit reticulocyte expression systems. The upper double bar represents the NEDD-2 gene and shows wild-type amino acids that were mutated to A residues. The fragments selected for amplification by PCR are represented by smaller double bars under NEDD. In the lower part, the gene fragments corresponding to the polypeptides of 17, 14, and 12 kD made in the SFV and reticulocyte systems are represented by single bars, and other processing products are shown by dotted lines. The starting site of the fragment of 17 kD (p20) and of the processing product of 30 kD is unknown and indicated with an X; likewise, the end of the fragment of 18 kD is indicated by a question mark.

Expression in the Semliki Forest Virus System

The pSFV-1 plasmid (Liljestrom and Garoff, 1991) was engineered to contain a unique ClaI site followed by an XbaI site just downstream from the SP6 promoter. The wild-type and the mutant genes were cloned between these sites (Fig. 1 *C*). In vitro RNA synthesis using pSFV-1 constructs and pSFV-helper-2 as templates, and coelectroporations into BHK-21 cells, were as described (Liljestrom and Garoff, 1991). For successful infection with virus stocks in BHK-21 or CHO cells, it was important that the cells be at 80% confluency. This was achieved by plating 2×10^5 cells in 35-mm tissue-culture plates on the day before infection. Infection, labeling with [^{35}S]methionine at various times after infection, and cell lysis in the presence of protease inhibitors were conducted according to Liljestrom and Garoff (1991). Samples corresponding to 4×10^4 cells per well were analyzed by SDS-PAGE in 4–20% gradient gels (Novex, San Diego, CA). The proteins were transferred electrophoretically to nitrocellulose membranes, and the membranes were exposed directly to x-ray films (X-Omat AR; Eastman Kodak Co., Rochester, NY) in pulse-chase experiments, or alternatively analyzed by Western blotting.

Western Blotting

After transfer, the nitrocellulose membrane was blocked at room temperature for 1 h in a PBS solution containing 5% dried milk and 0.2% Tween-20 (Bio Rad Laboratories, Hercules, CA). It was then immersed in a PBS solution containing the first antibody (i.e., polyclonal anti-p20) at a final concentration of 1.6 μg/ml, 2.5% dried milk, and 0.1% Tween-20 for 1 h on a shaker platform. The membrane was washed three times for 15 min each in a PBS solution containing 0.2% Tween-20, and then transferred to a PBS solution containing the second antibody (swine anti-rabbit IgG peroxidase), having otherwise the same composition as the first antibody. This incubation was for 2 h at room temperature on the shaking platform. After three cycles of washing as above, the membrane was developed with the enhanced chemiluminescence substrate (ECL; Amersham Intl., Little Chalfont, UK), as recommended, and exposed for a few seconds to Hyper film TM-ECL (Amersham Intl.).

Expression in the Rabbit Reticulocyte System

TNT coupled reticulocyte lysate system was purchased from Promega and used according to supplied instructions. Reaction mixtures (25 μl) containing 0.5 μg supercoiled plasmid DNA were incubated at 31°C in a thermomixer (Eppendorf North America, Inc., Madison, WI) without agitation. After incubation for 2 h, the samples were diluted 20 times in 20 mM Hepes, pH 7.0, and vortexed. Aliquots (5–10 μl) were mixed with equal volume of 2 × SDS-PAGE sample buffer and analyzed in 4–20% gradient gels. Gel transfer and autoradiography were as above.

SP73-his-NEDD-2

Vectors for fusing at the amino terminus a tag of 31 amino acids including 6 histidine residues followed by an epitope for a defined mAb (X-Press) and a proteolytic cleavage site for enterokinase are commercially available. By reassembling four synthetic oligonucleotides, we synthesized a DNA fragment incorporating the same characteristics, but with a coding capacity for 27 amino acids only, and restriction sites that facilitated integration into our expression systems. Thus, this ClaI-NdeI synthetic fragment was ligated to the NEDD-2 gene contained in an Nde-XbaI fragment, and the fusion gene was inserted between the unique ClaI and XbaI site of pSP73 (Fig. 1 *D*).

Results

Cloning and Mutagenesis

The NEDD-2 gene was cloned in our laboratory (M. Missotten) from a mouse thymus cDNA library (Stratagene, La Jolla, CA) using an oligonucleotide probe based on published data (Kumar et al., 1992). Compared to the gene described by Kumar et al. (1994), our clone contains an extra codon for leucine (CTC) at position 88 in the amino acid sequence. Appropriate restriction sites were created at both ends by PCR (Materials and Methods), and the full-length cDNA was cloned into plasmid vectors for expression in *E. coli*, neuronal cells, and Semliki Forest virus and rabbit reticulocyte systems (Fig. 1, *A–D*). Mutants in the Cys 320 or in various aspartate residues, and gene fragments including different combinations of p10 and p20 subunits, were prepared as described in Materials and Methods. They are shown in Fig. 2.

Survival Assays in Sympathetic Neurons

Sympathetic neurons depend on NGF for survival (Garcia et al., 1992). We first wanted to determine if overexpression of wild-type (WT) NEDD-2 and mutant derivatives in these neurons could trigger cell death. To test it, we cultured sympathetic neurons for 5 d in the presence of NGF and microinjected them with the pEE12 vector expressing separately each of the NEDD-2 mutants described above. 24 h after injection, survival of neurons was measured on the basis of morphological criteria and expressed as a percentage of the initial number of neurons (Garcia et al., 1992; Martinou et al., 1995). Fig. 3 shows that WT NEDD-2 triggered programmed cell death of neurons, whereas the mutant NEDD-2_{C320A} had no effect. Among the different mutants tested, D124A, D137A, D159A, and D347A behaved as WT NEDD-2, while D135A, D326A, D330A, and D333A abolished the killing activity of NEDD-2 as effectively as NEDD-2_{C320A}. Deletion of the first 137 amino acids (p20 + 10) also resulted in a loss of function of the protease. These results illustrate that the combination of mutagenesis and microinjection into sympathetic neurons

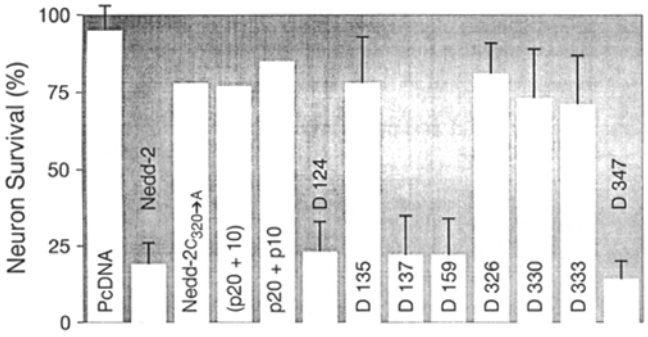

Figure 3. Biological test of neuron survival. Sympathetic neurons were cultured for 5 d in the presence of NGF. In each experiment, at least 100 neurons were microinjected with each DNA encoding either WT NEDD-2, NEDD-2_{C320A}, or the different mutant at aspartate (*D*) residues. 24 h later, neurons were analyzed for survival on the basis of morphological criteria. Results are mean ± SD for two or three experiments.

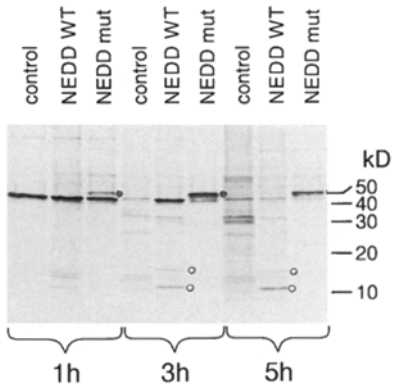

Figure 4. Pulse-chase labeling analysis of WT NEDD-2 and NEDD-2_{C320A} polypeptide in SFV. Virus stocks expressing a control gene (IL8 receptor), WT NEDD-2, and a gene mutant NEDD-2_{C320A} were used to infect CHO cells at high multiplicity of infection. The infected cells were pulse labeled with [^{35}S]methionine at various times after infection. Aliquots (10^4 cells) were lysed and submitted to SDS-PAGE (5–20% acrylamide gradient); the proteins were transferred to a nitrocellulose membrane and analyzed by radioautography as described in Materials and Methods. The size markers on the righthand side are 10 kD Protein Ladder (10–200 kD) from GIBCO BRL (Gaithersburg, MD). Unprocessed NEDD-2 in the NEDD-2 mut lanes (*filled circles*); two polypeptides between 10 and 20 kD in the lanes of NEDD WT (*open circles*). *NEDD WT*, wild-type NEDD-2; *NEDD mut*, NEDD-2_{C320A}. The origin of the strong band below 50 kD seen especially at early times is unknown.

can discriminate between functional and nonfunctional mutants.

Expression and Cleavage in the Semliki Forest Virus System

Semliki Forest virus (SFV) is an overexpression system in which viral RNA containing the gene of interest is introduced into a cell by electroporation, where it then drives its own replication, capping, and translation so that massive amounts of the protein are produced. Most protein synthesis is effectively shut down at late stage, and processing of the protein in question will clearly not have been subject to the same controls as in a normal cell. Despite these features, the system has been used successfully in our laboratory to produce various chemokine (Banks et al., 1995) and neurokinin receptors (Lundstrom et al., 1994, 1995) whose biological activities were demonstrated on the whole infected cells by correct ligand binding and agonist/antagonist, or ion trafficking, responses. These positive results encouraged us to test the technology with NEDD-2.

The SFV expression system was handled as described by Liljestrom and Garoff (1991). In a first set of experiments, the RNA transcribed in vitro from the pSFV-helper-2 vector was mixed with RNA transcribed from either pSFV1-NEDD-2 (WT) (Fig. 1 *C*) or pSFV1-NEDD-2_{C320A} mutant (mut), and the RNA mixtures were electroporated into BHK-21 cells. Successful electroporations were monitored by pulse labeling with [^{35}S]methionine, and the virus stocks were harvested 24 h later. Aliquots were used in pulse-chase experiments with [^{35}S]methionine (Materials and Methods) to compare the total labeled proteins made at various times after infection. A viral stock expressing a nonrelated protein (IL8-R) was included as control. The results are shown in Fig. 4. Strikingly, a protein of ~50 kD, corresponding to full-size NEDD-2, is detected in NEDD-2_{C320A} (mut) samples as early as 1 h after infection and still is the major component after 3 and 5 h. This full-size protein is not seen with WT NEDD-2, but lower molecular mass species are detected: one of ~35 kD, and two others between 10 and 20 kD. This result raises the interesting possibility that a direct correlation may exist between the apoptotic activity described in the preceding section and the ability of NEDD-2 to be cleaved in the SFV system.

In another experiment the same virus stocks were used to infect CHO cells, but pulse chase with [^{35}S]methionine was omitted. Instead, the nonradioactive cells were lysed at various times after infection and submitted to SDS-PAGE. The proteins were transferred to a nitrocellulose membrane and analyzed by Western blotting using the polyclonal antibodies raised against p20, as described in Materials and Methods. The results, shown in Fig. 5, confirm and extend the previous data. Full-size NEDD-2 was largely predominant in the NEDD-2_{C320A} samples, whereas smaller molecular mass species, mainly p20, were the major poplypeptides in WT NEDD-2. As expected, p10 was not detected with the anti-p20 antibody. In the WT NEDD-2 sample, two polypeptides of ~30 and 35 kD were quite abundant. Presumably, they represent specific cleavage intermediates that contain the p20 sequence. Smaller molecular mass species also appeared as minor components in NEDD-2_{C320A}, notably at ~35 kD. They may have arisen by cleavage at specific sites, but their inability to be converted into p20 would account for the lack of apoptotic activity observed with the mutant.

The aspartate mutants (Fig. 2) were also tested both in pulse-chase and Western blot studies. An example is shown in Fig. 6 where CHO cells were infected with SFV virus stocks prepared in parallel and expressing WT NEDD-2, NEDD-2_{C320A}, and four aspartate mutants. The cells were analyzed by Western blotting 3 and 6 h after infection. As expected, WT NEDD-2 and NEDD-2_{C320A} show the same patterns as in Fig. 5. Mutants D135A and

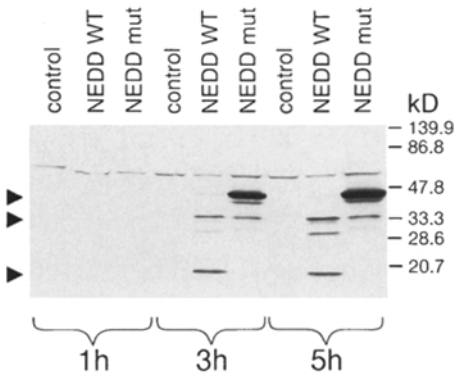

Figure 5. Western blot analysis of WT NEDD and NEDD-2_{C320A} polypeptides in SFV. Duplicates of the nonradioactive infected cells described in Fig. 4 were lysed at the indicated times after infection and submitted to SDS-PAGE (5–20% acrylamide gradient); the proteins were transferred to a nitrocellulose membrane, and the membranes were treated for Western blot analysis using the polyclonal antibodies against p20 as described in Materials and Methods. As size markers (*right*), low range prestained SDS-PAGE standards from Bio Rad Laboratories were used: phosphorylase B (*139.9 kD*), BSA (*86.8 kD*), ovalbumin (*47.8 kD*), carbonic anhydrase (*33.3 kD*), soybean trypsin inhibitor (*28.6 kD*), and lysozyme (*20.7 kD*). The arrows on the lefthand side point to the positions (from up to down) of uncleaved NEDD-2, the polypeptide of 35 kD, and the polypeptide (p20) migrating faster than the 20.7-kD size marker. *NEDD WT*, WT NEDD-2; *NEDD mut*, NEDD-2_{C320A}.

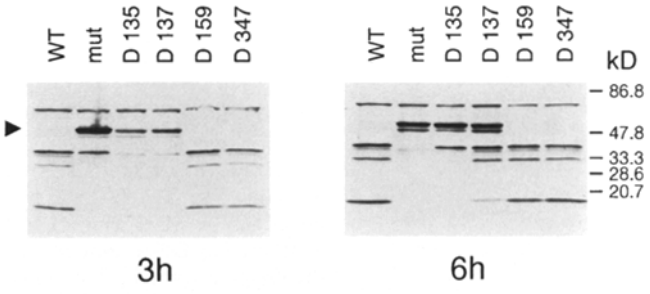

Figure 6. Comparative Western blot analysis of aspartate mutants in SFV. Virus stock expressing WT NEDD-2, NEDD-2_{C320A}, and four D to A mutants were used to infect CHO cells and analyzed by Western blots as described in Fig. 5. The size markers (*right*) are as in Fig. 5. The arrow (*left*) points to the position of uncleaved NEDD-2. *WT*, WT NEDD-2; *mut*, NEDD-2_{C320A}. The numbers indicate the mutants in which the corresponding aspartate has been replaced by an alanine residue.

D137A are poorly processed and resemble the NEDD-2_{C320A} pattern. Whereas D135A was shown (Fig. 3) to be inactive in the apoptotic test, D137A was active in this test. As can be seen in Fig. 6, however, D137A produces a low level of p20 6 h after infection. This would indicate that the apoptotic test in neuronal cells can respond to rather low levels of p20. Processing of D159A and D347A seemed indistinguishable from WT and produced p20 as early as 3 h after infection, and both had a WT phenotype in the apoptotic test.

The results described thus far argue that p20 is an essential component that correlates with biological activity as defined by the apoptotic assay in neuronal cells. The most convincing data derive from the Western blotting analyses using the anti-p20 antibodies. Since similar antibodies against p10 could not be obtained (Materials and Methods), analyses of the smaller subunit in the SFV system were limited to the examination of total radioactive proteins synthesized in pulse-chase experiments. As can be seen in Fig. 4, this type of analysis suffered from background problems that complicated unambiguous identification of the products.

Expression and Cleavage in the Rabbit Reticulocyte System

Rabbit reticulocyte is a coupled transcription/translation system in which a plasmid DNA containing the gene of interest under the control of a bacteriophage promoter is added to a cellular extract supplemented with the appropriate bacterial RNA polymerase. Because the balance of agonists or antagonists of any particular gene in the cellular extract is unknown, processing of the corresponding protein will, as in the SFV system, clearly not be subject to the same controls as in a normal cell. Due to the ease of handling and product detection, however, the system has been commonly tested, notably with the ICE-like CPP32 gene (Fernandes-Alnemri et al., 1994). In a preliminary experiment WT NEDD-2 and NEDD-2_{C320A} were introduced into the plasmid pSP73 (Fig. 1 *D*) and expressed in the coupled transcription/translation rabbit reticulocyte system (Promega) as described in Materials and Methods. Proteins synthesized in the presence of [^{35}S]methionine were qualitatively similar to those obtained with the same genes analyzed by pulse-chase labeling in the SFV system (Fig. 4). Since the background is lower in this system, interpretation of the results is easier. As observed with the SFV expression system, the mutant gene yielded a major polypeptide consistent with full-size NEDD-2, whereas the WT gene exhibited a number of smaller polypeptides, including the 35-kD polypeptide and the two polypeptides between 10 and 20 kD seen with the SFV system. This prompted us to adopt the reticulocyte system for confirming previous data and gaining information about p10 and the cleavage intermediates. To permit identification of the products, we first compared WT NEDD-2 to a derivative, his-NEDD-2, in which a tag of 27 amino acids containing six adjacent histidine residues had been fused in phase to the amino terminus of WT NEDD-2 (Materials and Methods). The results are shown in Fig. 7. Three polypeptides of 12, 14, and 17 kD, which have the same size in the NEDD-2 and his-NEDD-2 extracts, presumably do not include the amino terminus. In contrast, the polypeptides of 18, 35, and 50 kD migrate as larger products in his-NEDD-2, and therefore are likely to contain the amino-terminal sequence.

Size considerations suggest that the 18-kD polypeptide starts at the amino terminus and ends at a site upstream of the so-called p20 subunit, whereas the 35-kD protein is a cleavage intermediate that starts at the amino terminus and extends to a site downstream of p20 (Fig. 2). The 50-kD polypeptide is full-size, uncleaved NEDD-2. Its abundance relative to that of the cleavage products is significantly higher than when the same WT NEDD-2 gene was expressed in the SFV system (Fig. 4), stressing the influ-

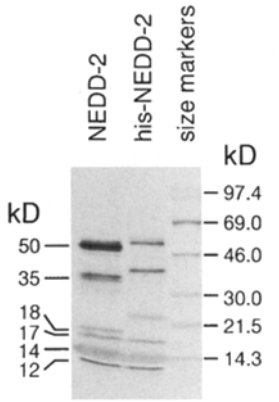

Figure 7. Identification of [^{35}S]methionine-labeled polypeptides containing the amino terminus of NEDD-2 in the rabbit reticulocyte expression system. Construction of his-NEDD-2 is described in Materials and Methods. WT NEDD-2 and his-NEDD-2 in SP73 (Fig. 1 *D*) were used as DNA templates in the coupled transcription–translation rabbit reticulocyte system and analyzed by SDS-PAGE (5–20% acrylamide gradient) as described in Materials and Methods. The proteins were transferred to a nitrocellulose membrane and exposed to x-ray film. The size markers (*right*) are the Rainbow ^{14}C-methylated protein molecular weight markers (Amersham Intl.), including BSA (*69.0 kD*), ovalbumin (*46.0 kD*), carbonic anhydrase (*30.0 kD*), trypsin inhibitor (*21.5 kD*), and lysozyme (*14.3 kD*). To facilitate further descriptions, the polypeptides made from NEDD-2 were named according to their apparent electrophoretic mobility (*left*).

ence that different test situations and/or cellular environments may exert on the efficiency of proteolytic cleavage. The product identifications and size assignments in Fig. 7 would imply that two of the three polypeptides identified between 10 and 20 kD represent the so-called p10 and p20 subunits, the presumed active components of NEDD-2. Combined with the results presented below in Fig. 8, we propose that these active subunits migrate as polypeptides of 12 and 17 kD, and that the 14-kD polypeptide is a fusion that contains p10 and a hypothetical linker region between p20 and p10 (Fig. 2).

Fig. 8 shows the polypeptides made in the reticulocyte system from WT NEDD-2, NEDD-2_{C320A}, and seven aspartate mutants analyzed in parallel. In this series, NEDD-2_{C320A}, D135A, D330A, and D333A were all without effect on neuron survival (Fig. 3). As can be seen, they all fail to produce both 12-kD and 17-kD products. In addition, NEDD-2_{C320A} and D135A seem equally inefficient in all proteolytic cleavages. Surprisingly, D137A, which was active in the apoptotic assay, produces some 35-kD polypeptides, but no detectable 12- and 17-kD polypeptides. Since a low level of p20 (17 kD) was detected with this mutant in SFV (Fig. 6), we cannot exclude the possibility that this apparent lack of cleavage is inherent in the reticulocyte system and is not paralleled in neuronal cells. A similar argument of system-dependent cleavage (or synthesis) may apply to D326. Inactive in the apoptotic assay, it fails to produce the 12-kD polypeptide, but seems to generate a low level of the 17-kD polypeptide.

In designing mutants D330A, D333A, and D347A, we had anticipated that the corresponding sites, lying in the area between p20 and p10, might play an important role in NEDD-2 processing. The following results entirely verified this expectation. Thus, the patterns observed with D330A and D333A support the hypothesis that they coincide with the cleavage site at the righthand side of p20. Based on the assignments in Fig. 2, lack of cleavage at this site would be expected to result in three alterations of the

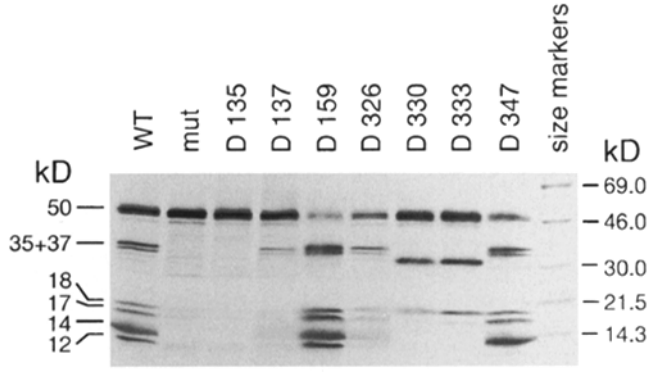

Figure 8. Mutant analysis in the rabbit reticulocyte system. WT NEDD-2, NEDD-2_{C320A}, and the indicated D to A mutants in SP73 were analyzed in parallel as described in Fig. 7. *WT*, WT NEDD-2; *mut*, NEDD-2_{C320A}.

WT pattern, namely, absence of the 35-kD product, fusion of 17- and 14-kD polypeptides to form a 30-kD product, and concomitant absence of 17- and 14-kD polypeptides. As seen in the figure, these alterations are indeed observed. In addition, the 12-kD product is not made, suggesting that it cannot be cleaved directly from 30 kD, but requires prior formation of the 14-kD polypeptide. The pattern observed with the D347A mutant supports and extends these interpretations. The mutant shares with WT NEDD-2 all the cleavage products except the 12-kD one (p10). Harboring intact D330, it produces, as expected, the 35-, 18-, 17-, and 14-kD polypeptides. The inability to generate the 12-kD product probably indicates that the mutated site coincides with the NH_2-terminal boundary of the p10 subunit.

Fig. 9 shows the results obtained with the gene fragments (Fig. 2) cloned into SP73 (Fig. 1 *D*) and analyzed as in Figs. 7 and 8. Fragment p(20 + 10) from T138 to T452 migrates with an apparent molecular mass of 35 kD and is thus larger than the corresponding 30-kD fragment described in Fig. 8 with D330A (D333A). It is not cleaved into the 12- and 17-kD products. Consistently, it did not show apoptotic activity in Fig. 3. Fragment p20, from T138 to D333A, migrates with an apparent molecular mass of about 20 kD, which is larger than the 17-D polypeptide

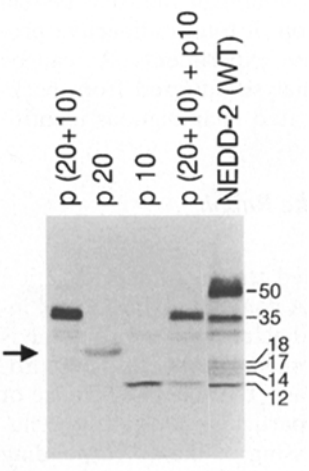

Figure 9. Analysis of PCR fragments in the rabbit reticulocyte system. The three PCR fragments p(20 + 10), p20, and p10 were cloned into SP73 and analyzed as in Figs. 7 and 8. Note that the PCR fragment p20 generates a polypeptide (*arrow*) that migrates significantly slower than the so-called p20 of 17 kD made from NEDD-2. Likewise, the PCR fragment p(20 + 10) produces a polypeptide migrating almost like the polypeptide of 35 kD made from NEDD-2.

corresponding to p20. This size assignment would locate the lefthand boundary of 17 kD at a site significantly distal relative to D135. In this context, mutant D159A failed to define this site by our biological activity and cleavage pattern criteria. We assume therefore that this site exists further downstream, possibly at aspartate residue D166 or D169. Fragment p10, from A348 to T452, migrates almost like a 12-kD polypeptide and is consistent with the assignment of D347 at the NH_2-terminal boundary of p10. Finally, a combination of the plasmids pSP73 expressing p(20 + 10) and p10 in the same reaction mixture did not affect the cleavage pattern.

Discussion

As a starting point for the present study, we knew the locations of intramolecular cleavage sites in ICE at four aspartate residues, D103, D119, D297, and D316 (Thornberry et al., 1992). However, because aspartate residues are frequent in the family of cysteine proteases, this information did not permit us to predict with certainty the corresponding sites in NEDD-2. Thus, it was necessary to generate a rather large number of mutants to identify these sites. Our task was greatly facilitated by the design of a PCR-based methodology that permitted rapid and efficient mutagenesis to obtain the desired derivatives (Materials and Methods).

Throughout the present study we have attempted to correlate activity and cleavage data using expression systems in which protein processing was likely to be subject to different controls. A priori, when extended to numerous examples, as was done here, this particular test situation might have quickly led to ambiguous interpretations. In fact, the internal consistency of almost all of the results based on these correlations argue that these system-borne differences were not so stringent as to invalidate the comparisons, at least qualitatively. Therefore, even if the chosen systems do not mimic exactly the in vivo situation, and if the precise role and requirement for each protein fragment is still not understood, our observations support the conclusion that NEDD-2 processing and apoptotic activity are linked phenomena. Thus, wild-type NEDD-2 had, as expected, an apoptotic effect in the neuronal cells (Fig. 3), and it was processed to the p20 and p10 subunits in the Semliki and reticulocyte systems (Figs. 4–9). In contrast, the cysteine mutant C320A showed no apoptotic activity in neuronal cells, as well as no processing in the Semliki Forest virus and rabbit reticulocyte systems. This confirmed the results of Kumar et al. (1994) concerning the role of this cysteine residue in apoptosis and further suggested a link between apoptotic activity and correct processing. Like C320A, the mutant D135A showed no apoptotic activity (Fig. 3) and no proteolytic processing (Figs. 6 and 8). The position of this site in NEDD-2 strongly suggests that it corresponds to D103 in ICE, defining one of the two cleavage sites upstream of p20. However, the fact that D135 mutant behaves like C320 mutant may lead to two alternative explanations: D135 is a cleavage site, or D135 mutation changes the overall structure of NEDD-2. The present data cannot distinguish between these two possibilities. Aspartate mutants D330A and D333A also lacked apoptotic activity (Fig. 3) and failed to produce p20 and p10 (Fig. 8). We assume that they define the cleavage site at the righthand side of p20 and correspond to the aspartate residue D297 in ICE.

It has been shown recently (Ramage et al., 1995) that the human ICE precursor of 45 kD made in *E. coli* as an insoluble protein (inclusion body) can be refolded, and that during the renaturation process it produces the p20 and p10 subunits without any additions other than reducing agents. The authors concluded that the maturation of precursor ICE leading to the active p20–p10 heterodimeric complex is an autocatalytic process. Maturation proceeds in a time-dependent manner, and examination of the intermediate products permits prediction about the temporal order of cleavages. Our results showing that the mouse NEDD-2 gene expressed in two widely different systems gives rise to the same type of intermediate and final products support these conclusions and suggest that, perhaps, other members of the cysteine protease family modulate their activity through protein processing.

Because no information was available about the cleavage specificity, we were uncertain if mutating aspartate residues at cleavage sites would result in cleavage at neighboring aspartate residues to produce novel derivatives, possibly with altered apoptotic activity. Our results argue that a high degree of specificity was retained. The most convincing examples are mutant D135A in the upstream region of p20, which shows no processing, and D330A (D333A) at the end point of p20, which shows only the uncleaved products expected after eliminating this site. It is interesting to note that while D135A did abolish all the cleavage events (same phenotype as C320A), mutant D330A and D333A did not prevent the cleavages at the sites upstream of p20 (Fig. 8). Whether or not this reflects an important feature in the mechanism of active protein formation from two precursor molecules is unknown.

In this study the aspartate residue that identifies the NH_2 terminus of p10 was convincingly shown to lie at position D347 (corresponding to D316 in ICE), as mutant D347A exhibits all the polypeptides made for WT NEDD-2, except p10, the polypeptide of 12 kD (Fig. 8). When tested in the biological neuronal assay, mutant D347A did promote an efficient apoptotic response indistinguishable from that of wild type. This raises the intriguing possibility that the polypeptide of 14 kD, a precursor of p10, would be capable of forming an active heterodimer complex with p20. Further studies with the D347 mutant will hopefully help to clarify this point.

In the present study three of the four autocatalytic cleavage sites in NEDD-2 have been identified. Thus, the dowstream aspartate residues D330 and D347 correspond to D297 and D316 in mouse ICE. Likewise, the upstream aspartate residue D135 in NEDD-2 corresponds to D103 in ICE. The residue that defines the starting site of p20 corresponding to aspartate D119 in ICE has escaped our analyses, but we know by size considerations that it exists at a position downstream of D159 (Fig. 2).

Together, our results establish a direct correlation between biological activity and proteolytic cleavage of Nedd-2 at specific sites. By showing differential effects of aspartate mutations on the overall cleavage patterns, these results also open ways to dissect the yet poorly understood mechanisms of subunit formation and assembly.

We thank Christopher Hebert for preparing the figures, Françoise Fichet and Nadine Huber for preparation of the manuscript, and Drs. Jonathan Knowles, Kinsey Maundrell, Jean-Jacques Mermod, and Eric Meldrum for helpful discussions and careful reading of the manuscript.

Received for publication 15 April 1996 and in revised form 31 July 1996.

References

Allet, B., M. Payton, R.J. Mattaliano, A.M. Gronenborn, G.M. Clore, and P.T. Wingfield. 1988. Purification and characterization of the DNA-binding protein Ner of bacteriophage Mu. *Gene (Amst.).* 65:259–268.

Ausubel, F.M., R. Brent, R.E. Kingston, J.G. Seidman, J.A. Smith, and K. Struhl. 1992. Short Protocols in Molecular Biology. Second edition. Harvard Medical School. Greene Publishing Associates and John Wiley & Sons, New York.

Banks, M., P. Graber, A.E.I. Proudfoot, C.Y. Arod, B. Allet, A.R. Bernard, E. Sebille, M. McKinnon, T.N.C. Wells, and R. Solari. 1995. Soluble interleukin 5 receptor alpha-chain binding assays: use for screening and analysis of IL5 mutants. *Anal. Biochem.* 230:321–328.

Bebington, C.R., and C.C.G. Hentschel. 1987. The use of vectors based on gene amplification for the expression of cloned genes in mammalian cells. In DNA Cloning. Volume III. D.M. Glover, editor. IRL Press, Oxford/Washington, DC. 163–189.

Bump, N.J., M. Hackett, M. Huguenin, S. Seshagiri, K. Brady, P. Chen, C. Ferenz, S. Franklin, T. Ghayur, P. Li et al. 1995. Inhibition of ICE family proteases by baculovirus antiapoptotic protein P35. *Science (Wash. DC).* 269: 1885–1888.

Ceretti, D.P., C.J. Kozloski, B. Mosley, N. Nelson, K.V. Ness, T.A. Greenstreet, C.J. March, S.R. Kronheim, T. Druck, L.A. Cannizaro et al. 1992. Molecular cloning of the interleukin-1β converting enzyme. *Science (Wash. DC).* 256: 97–100.

Duan, H., M. Chinnaiyan, P.L. Hudson, J.P. Wing, W.W. He, and V.M. Dixit. 1996. ICE-LAP-3, a novel mammalian homologue of the *Caenorhabditis elegans* cell death protein Ced-3 is activated during Fas- and tumor necrosis factor-induced apoptosis. *J. Biol. Chem.* 271:1621–1625.

Faucheu, C., A. Diu, A.W.E. Chan, A.M. Blanchet, C. Miossec, F. Hervé, V. Collard-Dutilleul, Y. Gu, R.A. Aldape, J.A. Lippke et al. 1995. A novel human protease similar to the interleukin-1 beta converting enzyme induces apoptosis in transfected cells. *EMBO (Eur. Mol. Biol. Organ.) J.* 14:1914–1922.

Fernandes-Alnemri, T., G. Litwack, and E.S. Alnemri. 1994. CPP32, a novel human apoptotic protein with homology to *Caenorhabditis elegans* cell death protein Ced-3 and mammalian interleukin 1β-converting enzyme. *J. Biol. Chem.* 269:30761–30764.

Fernandes-Alnemri, T., G. Litwack, and E.S. Alnemri. 1995*a*. Mch 2, a new member of the apoptotic Ced-3/ICE cysteine protease gene family. *Cancer Res.* 55:2737–2742.

Fernandes-Alnemri, T., A. Takahashi, R. Armstrong, J. Krebs, L. Fritz, K.J. Tomaselli, L. Wang, Z. Yu, C.M. Croce, G. Salveson et al. 1995*b*. Mch 3, a novel human apoptotic cysteine protease highly related to CPP 32. *Cancer Res.* 55:6045–6052.

Gagliardini, V., P.A. Fernandez, R.K.K. Lee, H.C.A. Drechsler, R.J. Rotello, M.C. Fishman, and J. Yuan. 1994. Prevention of vertebrate neuronal death by the crmA gene. *Science (Wash. DC).* 263:826–828.

Garcia, I., I Martinou, Y. Tsujimoto, and J.C. Martinou. 1992. Prevention of programmed cell death of sympathetic neurons by the bcl-2 protooncogene. *Science (Wash. DC).* 258:302–304.

Gu, Y., J. Wu, C. Faucheu, J.L. Lalanne, A. Diu, D.J. Livingston, and M.S.S. Su. 1995. Interleukin-1 beta converting enzyme requires oligomerization for activity of processed forms in vivo. *EMBO (Eur. Mol. Biol. Organ.) J.* 14: 1923–1931.

Kamens, J., M. Paskind, M. Huguenin, R.V. Talanian, H. Allen, D. Banach, N. Bump, M. Hackett, C.G. Johnston, P. Li et al. 1995. Identification and characterization of ICH-2, a novel member of the interleukin-1-beta-converting enzyme family of cysteine proteases. *J. Biol. Chem.* 270:15250–15256.

Kumar, S., Y. Tomooka, and M. Noda. 1992. Identification of a set of genes with developmentally down-regulated expression in the mouse brain. *Biochem. Biophys. Res. Commun.* 185:1155–1161.

Kumar, S., M. Kinoshita, M. Noda, N.G. Copeland, and N.A. Jenkins. 1994. Induction of apoptosis by the mouse Nedd-2 gene which encodes a protein similar to the product of the *Caenorhabditis elegans* cell death gene Ced-3 and the mammalian IL-1β converting enzyme. *Genes & Dev.* 8:1613–1626.

Liljestrom, P., and H. Garoff. 1991. A new generation of animal cell expression vectors based on the Semliki Forest virus replicon. *Biotechnology (NY).* 9: 1356–1361.

Lundstrom, K., A. Mills, G. Buell, E. Allet, N. Adami, and P. Liljestrom. 1994. High-level expression of the human neurokinin-1 receptor in mammalian cell lines using the Semliki Forest virus expression system. *Eur. J. Biochem.* 224:917–921.

Lundstrom, K., A. Vargas, and B. Allet. 1995. Functional activity of a biotinylated human neurokinin-1 receptor fusion expressed in the Semliki Forest virus system. *Biochem. Biophys. Res. Commun.* 208:260–266.

Maniatis, T., E.F. Fritsch, and J. Sambrook. 1982. Molecular Cloning. A Laboratory Manual. Cold Spring Harbor Laboratory, Cold Spring Harbor, NY. 545 pp.

Martin, S.J., and D.R. Green. 1995. Protease activation during apoptosis: death by a thousand cuts? *Cell.* 82:349–352.

Martinou, I., P.A. Fernandez, M. Missoten, E. White, B. Allet, R. Sadoul, and J.C. Martinou. 1995. Viral proteins E1b19K and p35 protect sympathetic neurons from cell death induced by NGF deprivation. *J. Cell Biol.* 128:201–208.

Munday, N.A., J.P. Vaillancourt, A. Ali, F.J. Casano, D.K. Miller, S.M. Molineaux, T.T. Yamin, V.L. Yu, and D.N. Nicholson. 1995. Molecular cloning and pro-apoptotic activity of ICE rel II and ICE rel III, members of the ICE/Ced-3 family of cysteine proteases. *J. Biol. Chem.* 270:15870–15876.

Nicholson, D.N., A. Ali, N.A. Thornberry, J.P. Vaillancourt. C.K. Ding, M. Gallant, Y. Gareau, P.R. Griffin, M. Labelle, Y.A. Iazebnik et al. 1995. Identification and inhibition of the ICE/Ced-3 protease necessary for mammalian apoptosis. *Nature (Lond.).* 376:37–43.

Ramage, P., D. Cheneval, M. Chvei, P. Graff, R. Hemmig, R. Heng, H.P. Kocher, A. Mackenzie, K. Memmert, L. Revesz et al. 1995. Expression, refolding, and autocatalytic proteolytic processing of the interleukin-1 beta converting enzyme precursor. *J. Biol. Chem.* 270:9378–9383.

Tewari, M., L.T. Quan, K. O'Rourke, S. Desnoyers, Z. Zeng, D.R. Beidler, G.G. Poirier, G.S. Slavesen, and V.M. Dixit. 1995. Yama/CPP32 beta, a mammalian homologue of Ced-3, is a Crm A-inhibitable protease that cleaves the death substrate poly(ADP-ribose) polymerase. *Cell.* 81:801–809.

Thornberry, N.A., H.G. Bull, J.R. Calaycay, K.T. Chapman, A.D. Howard, M.J. Kostura, D.K. Miller, S.M. Molineaux, J.R. Weidner, J. Aunins et al. 1992. A novel heterodimeric cysteine protease is required for interleukin-1 beta processing in monocytes. *Nature (Lond.).* 356:768–774.

Walker, N.P., R.V. Talanian, K.D. Brady, L.C. Dang, N.J. Bump, C.R. Ferenz, S. Franklin, T. Ghayur, M.C. Hackett, L.D. Hammill et al. 1994. Cristal structure of the cysteine protease interleukin-1 beta-converting enzyme: a (p20/p10)2 homodimer. *Cell.* 78:343–352.

Wang, L., M. Miura, L. Bergeron, H. Zhu, and J. Yuan. 1994. Ich-1, an ICE/Ced-3-related gene, encodes both positive and negative regulators of programmed cell death. *Cell.* 78:739–750.

Wilson, K.P., J.A.F. Black, J.A. Thomson, E.E. Kim, J.P. Griffith, M.A. Navia, M.A. Murcko, S.P. Chambers, R.A. Aldape, S.A. Raybuck et al. 1994. Structure and mechanism of interleukin-1β converting enzyme. *Nature (Lond.).* 370:270–274.

Xue, D., and H.R. Horvitz, 1995. Inhibition of the *Caenorhabditis elegans* cell-death protease Ced-3 by a Ced-3 cleavage site in baculovirus p35 protein. *Nature (Lond.).* 377:248–251.

Yuan, J. 1995. Molecular control of life and death. *Curr. Opin. Cell Biol.* 7:211–214.

Yuan, J., S. Shaham, S. Ledoux, H.M. Ellis, and H.R. Horvitz. 1993. The *C. elegans* cell death gene ced-3 encodes a protein similar to mammalian interleukin-1 beta-converting enzyme. *Cell.* 75:641–652.